Development and validation of an oxidative stress-related prognostic signature in osteosarcoma: A combination of molecular experiments and bioinformatics

BIN XIE*, SHIYONG TAN*, CHAO LI* and JUNYANG LIANG

Second Department of Spinal Surgery, Weihaiwei People's Hospital, Weihai, Shandong 264200, P.R. China

Received February 1, 2023; Accepted April 21, 2023

DOI: 10.3892/ol.2023.13865

Abstract. Osteosarcoma (OS) is one of the most prevalent malignancies with a bad prognosis. Oxidative stress is closely associated with various type of cancer. The present study aimed to establish an oxidative stress-related gene prognostic signature. Supported by The Cancer Genome Atlas and Gene Expression Omnibus, the least absolute shrinkage and selection operator regression, Cox regression, receiver operating characteristic curves and Kaplan-Meier survival analysis were used to construct and validate a prognostic signature and the derived risk score. Tumor microenvironment scores and immune infiltration levels in OS were calculated. Correlation between these parameters and risk score was analyzed. In addition, single analysis of each hub gene was performed. Finally, a series of molecular experiments was used to detect the role of MAP3K5 (one of the hub genes) in OS. A total of five genes most associated with OS prognosis were identified as independent predictors, namely catalase (CAT), mitogen-activated protein kinase 1 (MAPK1), glucose-6-phosphate dehydrogenase (G6PD), mitogen-activated protein kinase kinase kinase 5 (MAP3K5) and C-C motif chemokine ligand 2 (CCL2). Based on the signature, higher risk score indicated poorer prognosis. Nomogram performed well and reliably predicted 3- and 5-year survival rate in OS. Patients with increasing risk scores had higher tumor purity and lower immune infiltration levels. Compared with an osteoblast cell line, the expression of CAT, CCL2, MAPK1 and G6PD was upregulated and MAP3K5 was downregulated. MAP3K5 inhibited cellular proliferation and motility, promoted cellular apoptosis and induced reactive oxygen species generation. Overall, the signature could effectively predict the prognosis of patients with OS and were expected to be potential biomarkers. And it provided new ideas for understanding the interactions between oxidative stress and OS.

Correspondence to: Dr Junyang Liang, Second Department of Spinal Surgery, Weihaiwei People's Hospital, 70 Qingdaobei Road, Weihai, Shandong 264200, P.R. China
E-mail: whwjzwk@163.com

*Contributed equally

Key words: osteosarcoma, oxidative stress, prognostic signature, MAP3K5

Introduction

Osteosarcoma (OS) is one of the most commonly encountered malignancies in the world, with an occurrence rate of one to four in a million (1,2). It is more commonly noted in the epiphysis of young bones. OS is a highly invasive disease. It easily spreads and metastasizes through the bloodstream during the initial stages of its development and the resulting metastases to the lungs are the primary reasons of patient mortality (3). Despite significant progress in the diagnosis and treatment of OS, the survival rate is low and the prognosis is poor. Currently, it is considered that the majority of cases with OS are developed by interactions between the environment and the cytogenetic material, with oxidative stress possibly being one of the main attributing factors (4,5).

Oxidative stress is a physiological disorder induced by an unbalance between the production of free radicals during oxidation and the ability to scavenge them; it is characterized by increased levels of reactive oxygen species (ROS). Increased ROS production has been found in a variety of tumors to date (6,7). Elevated levels of ROS have long been considered to be a carcinogenic factor as increased ROS can damage cellular genetic material (8,9). However, recent studies have reported that ROS can act as a signal in tumors, blocking cancer differentiation (10,11). The importance of ROS in the regulation of cellular function cannot be overstated.

It has been shown that the generation of ROS is critical in regulating osteocyte function; in addition, the pathophysiology of mineralized tissues is affected by oxidative stress (12). The role of oxidative stress in OS has rarely been reported in the literature. It has been shown that OS cell proliferation and migration are regulated in part by redox-activated sodium-hydrogen antiporter 1 (13). Oxidative stress induced by low-dose doxorubicin promotes the invasiveness of OS (14). Therefore, the role of oxidative stress in OS remains to be further explored. It is important to build a prognostic signature for OS management by screening for

oxidative stress-related genes (OXSRGs) that are associated with OS prognosis.

In the present study, an OXSRG signature was identified to be associated with OS prognosis following the analysis of data from The Cancer Genome Atlas (TCGA). The interaction between this signature and the tumor microenvironment (TME) was subsequently investigated. In addition, molecular analysis was performed to further explore the role of OXSRGs in OS.

Materials and methods

Acquisition of hub OXSRGs associated with OS prognosis. The RNA sequencing (RNA-seq) data and the clinical characteristics of OS were obtained from the TARGET program of the TCGA database (https://portal.gdc.cancer.gov/). The keywords used for the searching data were 'transcriptome profiling', 'gene expression quantification', 'RNA-seq' and 'bones, joints, and articular cartilage of limbs'. Following exclusion of the patients with unknown survival status, data from 84 cases were included. This dataset was used as the training cohort. GSE21257, which was used as an external validation set, was a dataset of 53 OS samples with prognostic information obtained from the Gene Expression Omnibus database.

The GeneCards website was searched with the keyword 'oxidative stress' and the pertinent genes were obtained. The genes with a score ≥7 were selected for the next step of the univariate COX regression analysis. The least absolute shrinkage and selection operator regression (LASSO) with default parameters was used for subsequent screening of the hub OXSRGs.

Functional enrichment analysis of hub OXSRGs. The Spearman test was used to calculate the correlation between the expression levels of the hub OXSRGs. Furthermore, a network of hub OXSRGs and their 20 co-expression genes was analyzed via GeneMANIA (15). In addition, enrichment analyses of the hub OXSRGs in Gene Ontology (GO) and Kyoto Encyclopedia of Genes and Genomes (KEGG) were performed using the clusterProfiler package (16).

Construction and validation of the prognostic signature. The risk score was calculated as follows: Risk score=(Exp=expression level; Coe=regression coefficient). To assess the probability of survival in OS, a nomogram was constructed, combining clinical characteristics and the prognostic signature. The calibration curves were used for assessing the nomogram.

The patients were separately classified into a low-risk and a high-risk group according to the median value of the risk score. Kaplan-Meier (KM) survival analysis was used to estimate the overall survival of the two groups. Receiver operating characteristic (ROC) curves were performed to calculate the sensitivity and specificity. These analyses were repeated in the validation dataset. Finally, COX regression was used to determine whether the signature was an independent prognostic factor.

In addition, KM survival analysis and ROC curves were used for each of the hub genes to assess the significance of each single gene.

Analysis of TME. Estimate package was applied to calculate the TME scores and tumor purity (17). The Wilcoxon rank sum test was used to analyze the differences between two groups. In addition, the correlation between the risk score and the tumor purity was assessed by the Spearman test.

Single sample gene set enrichment analysis was applied to explore the immune infiltration levels in OS. Pearson correlation was used to assess the correlation between risk score and immune infiltration.

Identification and functional enrichment analysis of differentially expressed genes (DEGs). The comparison of low- and high-risk groups with the limma package resulted in the identification of DEGs in the high-risk group (18). When the DEGs were obtained, false discovery rate (FDR)<0.05 and |log2FC|>2 was considered to indicate a statistically significant difference. The Protein-Protein Interaction (PPI) network, which was based on DEGs, was constructed by the STRING database. The confidence level was set as a combined score >0.9. Finally, a functional enrichment analysis of DEGs was performed in KEGG and GO.

Cell culture and transfection. Three OS cell lines (MG63, U2OS, and HOS) and one osteoblast cell line (hFOB1.19) were used in this study. The OS cell lines were purchased from Zhong Qiao Xin Zhou Biotechnology Co. The osteoblast cell line (hFOB1.19) was purchased from Procell Life Science & Technology Co., Ltd. Three human OS cell lines (HOS, MG63, and U2OS) were maintained in a humidified incubator at 37˚C in the presence of 5% CO2, while the human osteoblast cell line (hFOB1.19) was maintained at 34˚C. MG63, U2OS, and HOS cells were cultured in MEM complete medium and hFOB1.19 cells were cultured in DMEM/F-12 complete medium. All complete media contained 10% FBS (Gibco; Thermo Fisher Scientific, Inc.) and 1% antibiotics (100 units/ml penicillin and 100 units/ml streptomycin).

A mitogen-activated protein kinase kinase kinase 5 (MAP3K5) overexpression plasmid was purchased from Shanghai GeneChem Co., Ltd. and used to infect HOS cells according to the manufacturer's protocol. The name of the plasmid backbone for the overexpression vector was CMV enhancer-MCS-SV40-puromycin. The control was empty plasmid, which was constructed using the same method but without the target gene inserted.

Total RNA was extracted from cells using TRIzol® reagent (Thermo Fisher Scientific, Inc.) according to the instructions of the manufacturer. PCR was subsequently performed to determine the mRNA expression levels of the genes according to previous studies (19). β-actin was set as an internal control and the relative gene expression was calculated by the $2^{-\Delta\Delta Cq}$ method. The sequences of primers were included in Table SI.

Detection of the effect of MAP3K5 on OS cells. The cells were seeded at a density of $1x10^3$ cells/well in a 96-well plate. A total of 10 μl Cell Counting Kit-8 (CCK-8) reagent was added at specific timepoints. Following incubation at 37˚C for 1 h, the optical density was measured at 450 nm.

The EdU Detection Kit (Guangzhou RiboBio Co., Ltd.) was used to assess the fraction of DNA-replicating cells, which represented the cell proliferative status.

Table I. Demographic and clinical characteristics of patients.

Characteristics	TARGET cohort (n=84)	GSE21257 (n=53)
Sex (male/female)	47/37	34/19
Age (years)	14.98±4.78	18.71±12.20
Survival status (alive/dead)	55/29	30/23
Average survival time (months)	76.21±68.81	38.17±40.45

The wound healing assays were performed by using a sterile pipette tip to scratch and form a gap when cells were completely confluent in the 6-well plate. Subsequently, serum-free medium was added. Following incubation for 24 h, the gap was imaged.

Transwell assays were performed according to a previous study (20). Initially, $1x10^4$ cells per group were inoculated in the upper chamber. Following 24 h of cell incubation, the cells in the bottom chamber were fixed, stained, and photographed.

The cell suspensions were made in a phosphate-buffered saline solution. Annexin V-FITC Apoptosis Detection Kit (Vazyme Biotech Co., Ltd.) and flow cytometry were used to detect apoptosis.

According to the manufacturer's protocol, ROS generation was detected via a Reactive Oxygen Species Assay Kit (Beyotime Institute of Biotechnology). The incremental production of ROS was expressed as a percentage of control.

Statistical analysis. The present study was based on the R software (version 4.1.2) to analyze the data and generate graphs. All experiments were performed at least three times independently. Continuous variables were expressed using the mean ± standard deviation. Flexible statistical methods were used in the statistical analysis. $P<0.05$ was considered to indicate a statistically significant difference.

Results

Identification of hub OXSRGs and functional enrichment analysis. The data were collated to obtain a gene expression matrix containing 84 patients, of whom 55 survived and 29 did not. The pertinent information is presented in Table I. Following screening, 807 genes associated with oxidative stress were obtained from the GeneCards website. Subsequently, 17 genes associated with prognosis of OS were obtained by univariate COX regression (Fig. 1A). The five most powerful prognostic genes were identified by LASSO regression (Fig. 1B and C).

The data indicated a significant correlation in the expression levels between the five hub OXSRGs (Fig. 2A). GeneMANIA revealed that mitogen activated protein kinase 1 (MAPK1) and MAP3K5 were involved in several biological functions related to oxidative stress, such as response to oxidative stress and ROS and cellular response to oxidative radicals (Fig. 2B). The GO and KEGG enrichment results also indicated that hub OXSRGs were involved in a variety of oxidative stress-related pathways and functions including the forkhead box signaling pathway. Notably, certain hub genes were also associated with inflammatory and immune-related pathways, such as the IL-17 and the TNF signaling pathways (Fig. 2C-F).

Establishment of the prognostic signature based on five hub OXSRGs. Regression coefficients were assigned to the formula to calculate a combined risk score for the five genes to assess the prognosis of patients. Patients were grouped according to the median risk score (Fig. 3A). The risk score was higher in patients with poor survival as shown in the scatter plot (Fig. 3B). The heat map indicated the expression profiles of the five hub genes in the training cohort (Fig. 3C). Finally, a nomogram including age, sex, and the risk score based on the signature was successfully constructed (Fig. 3D). The calibration plots demonstrated that the predictive results of the nomogram were highly consistent with the actual observations (Fig. 3E).

A significant difference was noted in the survival probability between the two groups ($P<0.001$; Fig. 3F). The time-dependent ROC curves suggested optimal specificity and sensitivity for the prognostic evaluation of the signature in patients with OS (Fig. 3G). The data from the validation set indicated that the prognostic signature remained highly stable (Fig. 3H and I).

Finally, the univariate and multivariate COX regression analyses were used to investigate the predictive power of the signature. The results of both analyses indicated that the risk score was an independent prognostic factor for patients with OS ($P<0.001$; Fig. 3J and K). The coefficients of five hub OXSRGs are depicted (Fig. 3L).

Correlation analysis between risk score and TME. The results indicated that the high-risk group exhibited lower stromal scores, immune scores, and higher tumor purity, compared with those of the low-risk group (Fig. 4A and B). Scatter plot analysis indicated a positive correlation between the risk score and the tumor purity ($R=0.558$; Fig. 4C).

The butterfly diagram illustrated the correlation between the risk score and the immune infiltration phenotype (Fig. 4D). The risk score was negatively correlated with the level of infiltration of almost all immune cells and immune-related functions ($P<0.05$). The aforementioned results indicated that the prognostic signature could assess the immune status of patients with OS to a certain extent.

Functional enrichment analysis of DEGs. The data indicated that in the high-risk group, the majority of the genes were downregulated (Fig. 5A). The PPI network demonstrated the interactions between these DEGs (Fig. 5B).

GO and KEGG enrichment analysis revealed that these DEGs were significantly enriched in a large number of pathways. For instance, in KEGG, DEGs were involved in the NF-κB signaling pathway (Fig. 5C). This pathway has been

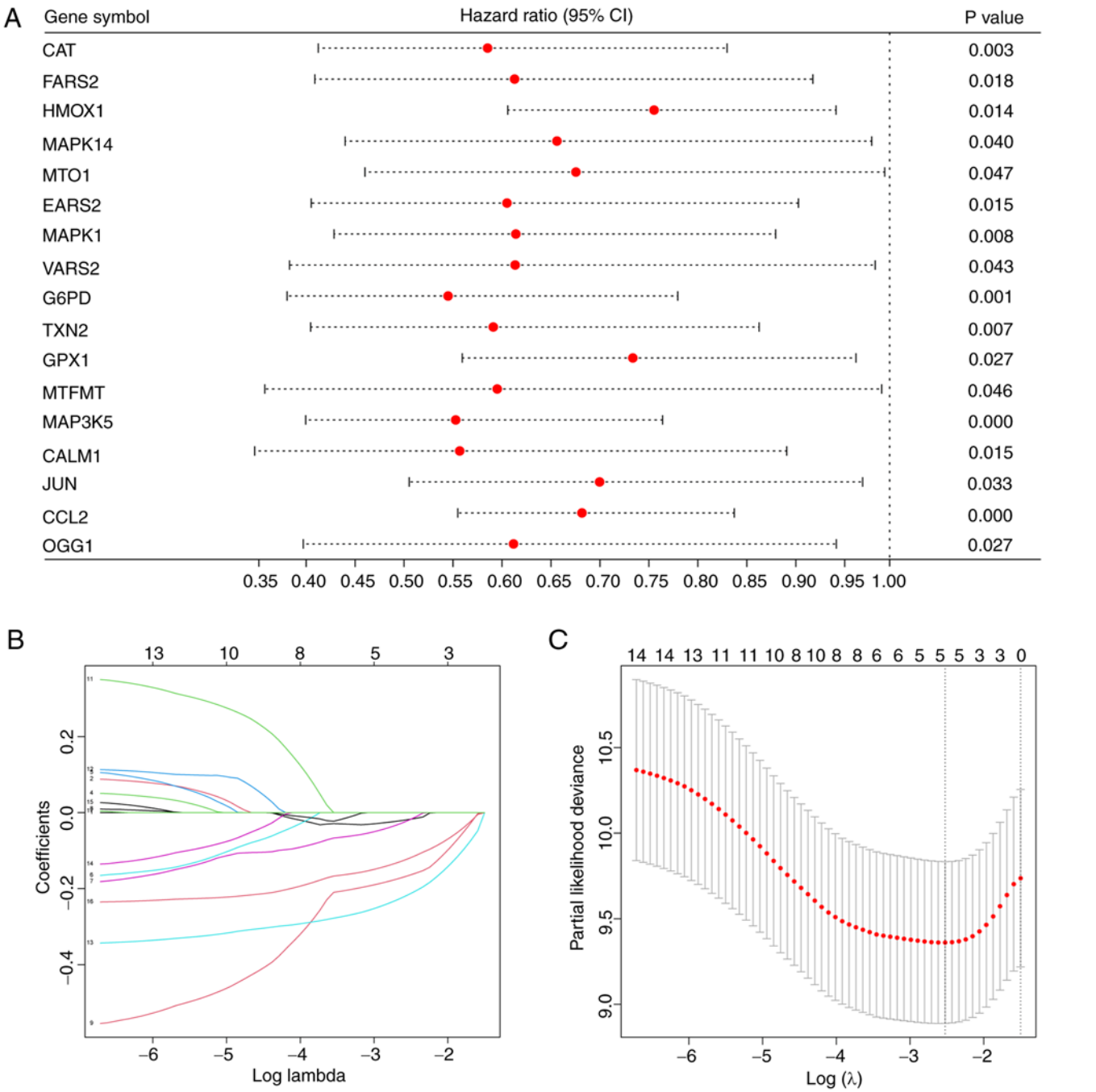

Figure 1. Screening of hub OXSRGs. (A) Forest plot showed all OXSRGs associated with prognosis in osteosarcoma. (B) Least absolute shrinkage and selection operator regression coefficient profiles were depicted. (C) Optimal values of the penalty parameter were defined by 1,000-round cross-validation. OXSRGs, oxidative stress-related genes.

demonstrated to regulate the amount of intracellular ROS and to be involved in a variety of immune processes (21,22). GO enrichment analysis indicated regulation of T cell activation and regulation of the inflammatory response, and other immune-related pathways (Fig. 5D-F). Table II describes the detailed information related to the five hub genes.

Analysis of single gene. In Fig. 6A and B, single-gene analysis indicated that all hub OXSRGs with the exception of MAPK1 (P=0.13) were significantly associated with patient prognosis. ROC curves indicated the satisfactory predictive value of hub OXSRGs.

In Fig. 6C, compared with hFOB 1.19, the mRNA levels of chemokine ligand 2 (CCL2), catalase (CAT), MAPK1 and glucose-6-phospate dehydrogenase (G6PD) were significantly elevated in the OS cell line, whereas the expression levels of MAP3K5 were significantly decreased (P<0.05). In the five hub genes, the absolute values of the regression coefficients of MAP3K5 were the highest. In addition, MAP3K5 was the only gene that was downregulated in the OS cell lines. Therefore, the role of MAP3K5 was assessed in OS.

MAP3K5 inhibited the OS cell and induced ROS generation. MAP3K5 expression was successfully upregulated in HOS

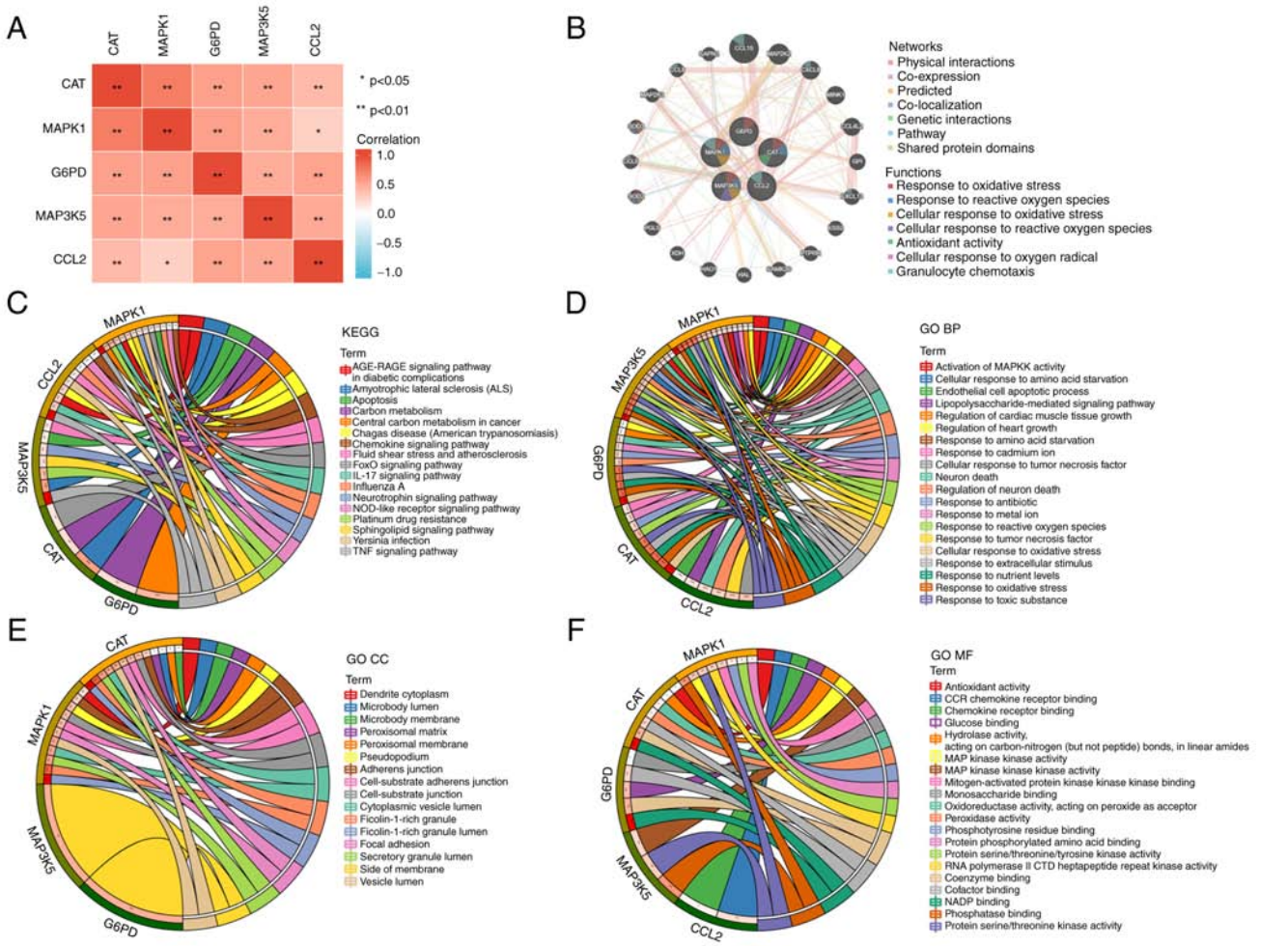

Figure 2. Function analysis of hub OXSRGs. (A) Correlation of hub OXSRGs expression. (B) Hub OXSRGs and their co-expression genes were analyzed using GeneMANIA. Functional enrichment analysis of hub OXSRGs in (C) KEGG and (D-F) GO including (D) BP, (E) CC and (F) BP, biological processes; CC, cellular components; MF, molecular functions; OXSRGs, oxidative stress-related genes; KEGG, Kyoto Encyclopedia of Genes and Genomes; GO, Gene Ontology.

cells (Fig. 7A). CCK-8 assays and EdU staining revealed that overexpression of MAP3K5 inhibited cell proliferation (Fig. 7B and C). By using wound healing assays, it was shown that MAP3K5 attenuated cell motility (Fig. 7D). Moreover, transwell assays further validated these findings (Fig. 7D). The data from flow cytometry analysis revealed that MAP3K5 caused increased apoptosis in the cells (Fig. 7F). Finally, higher ROS generation was detected in HOS cells following MAP3K5 overexpression (Fig. 7G). The aforementioned data indicated that MAP3K5 exhibited inhibitory effects on OS cells, which may be mediated via ROS production.

Discussion

OS is a frequent type of primary orthopedic malignancy. As the clinical significance of specific molecular markers is continuously explored, accumulating studies have concluded that molecular markers can predict tumor prognosis. A high number of predictors and therapeutic targets are being identified. The usage of risk models to predict tumor prognosis is becoming increasingly accepted. However, no studies have been conducted to construct an effective prognostic signature based on OXSRG in OS. In the present study, OXSRGs were studied using a bioinformatics approach and their prognostic power for OS was demonstrated. Ultimately, a five-gene signature (CAT, MAPK1, G6PD, MAP3K5, and CCL2) was constructed. The combination of clinical characteristics and the signature created a nomogram with optimal applicable value.

Regulation of oxidative stress is an important factor in tumor development and in the response to antitumor therapy (23). One of the characteristics of tumors is the Warburg effect and the high levels of oxidative stress (24,25). High ROS levels may inhibit tumorigenesis. However, ROS can also promote tumor formation through the induction of DNA mutations and pro-oncogenic signaling pathways (26). This paradox has important implications for developing therapies against cancer by regulating ROS levels. Therefore, the advantage of the present study was that it improved the understanding of oxidative stress in OS. In addition, the present study also provided suggestions for treating OS via regulation of oxidative stress.

A study by Babior *et al* reported that human phagocytes (mainly neutrophils and macrophages) utilized membrane NADPH oxidase to produce large amounts of O2, which was subsequently decomposed by superoxide dismutase into H2O2 and oxygen (27). Subsequently, the study examining the balance between oxidative and antioxidant systems in

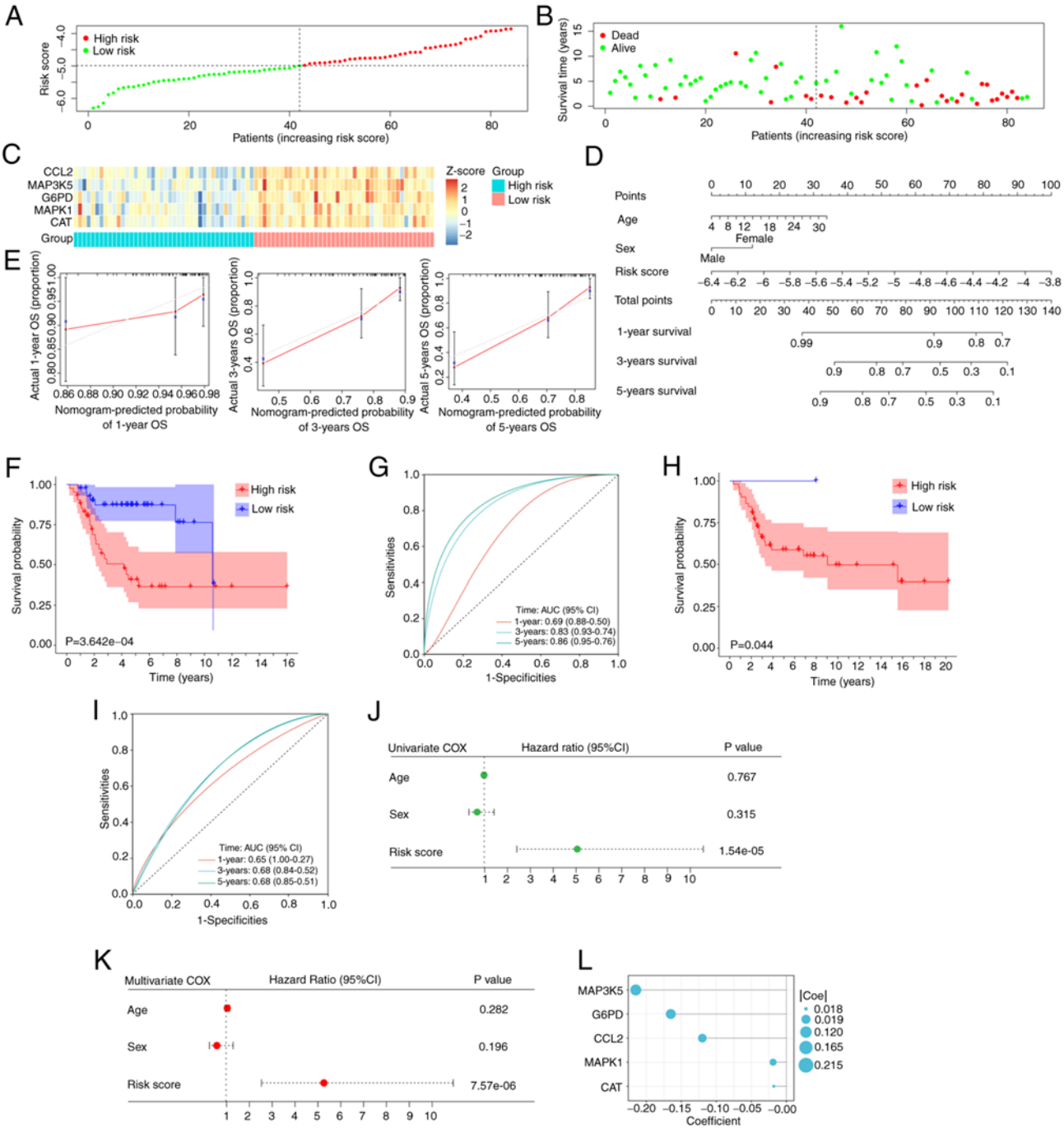

Figure 3. Construction and validation of the nomogram. (A) Risk score distribution and (B) survival status of patients with osteosarcoma. (C) Expression profiles of the five hub OXSRGs in TARGET cohort. (D) Nomogram consisted of age, sex and risk score based on the five hub OXSRGs signature. (E) Calibration curve for validation of the nomogram for estimating the survival of osteosarcoma patients at 1, 3 and 5 years. (F) Kaplan-Meier survival analysis of patients in TARGET cohort. (G) ROC curves demonstrated the predictive prognostic value of risk score. Validation of the nomogram in GSE21257 including (H) Kaplan-Meier survival analysis and (I) ROC curves. Forest plot showed risk score was an independent prognostic factor, with green indicated (J) univariate COX regression and (K) red indicated multivariate COX regression. (L) Regression coefficients of hub OXSRGs that made up the signature. OXSRGs, oxidative stress-related genes; ROC, receiver operator curves.

physiological and pathophysiological conditions has had a significant influence on the scientific field of immunology. It is now becoming more and more apparent that ROS has an important role in the immune system and that it is closely associated with various aspects of the immune response, such as immune cell interactions and activation, immunosuppression, and host defense (28). The interaction between immune function and tumors has received increasing attention and a large number of studies have been reported in the literature. Mifamurtide is an immune adjuvant, which has been at the forefront of OS treatment; however, there is a lack of large-scale clinical trials to demonstrate its efficacy and safety. Therefore, Kansara *et al* have suggested that the understanding of the relationship between bone tumors and immune function is still in its infancy (1). The data of the present study indicated a significant difference in the immune

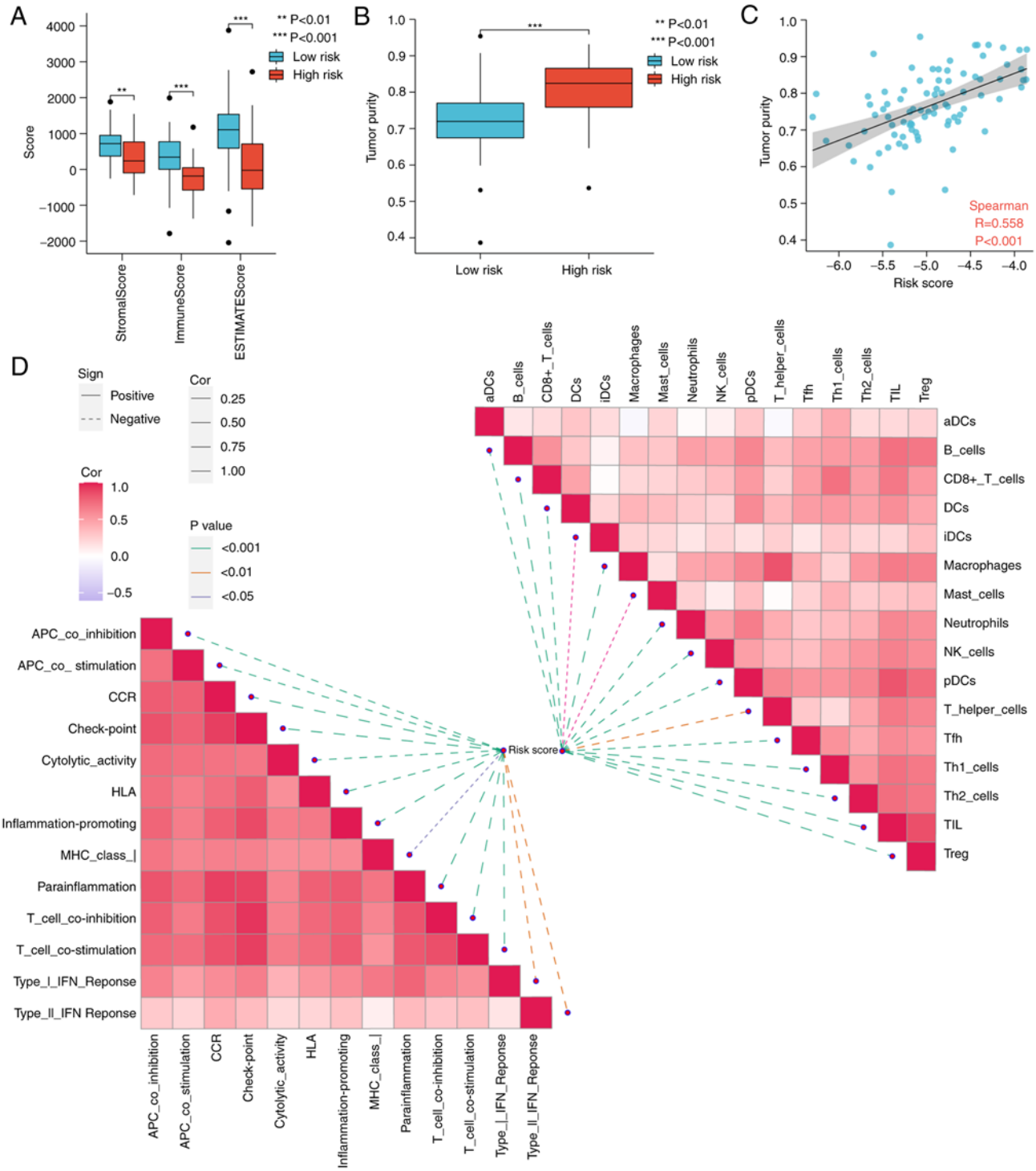

Figure 4. Tumor microenvironment analysis. (A) Box plots demonstrated that the tumor microenvironment scores were higher in the low-risk group than in the high-risk group. (B) Tumor purity was significantly higher in the high-risk group than in the low-risk group. (C) Positive correlation between tumour purity and risk score. (D) Butterfly diagram demonstrated the correlation between risk score and immune infiltration of osteosarcoma. **P<0.01 and ***P<0.001. aDC, activated dendritic cells; DC, dendritic cells; iDCs, immature dendritic cells; pDCs, plasmacytoid dendritic cells; Tfh, T follicular helper cells; Th, T helper cells; TIL, tumor-infiltrating lymphocytes; Treg, regulatory T cells.

infiltration between the high-risk and low-risk groups. In the highly risk scores, both immune scores and levels of immune infiltration were significantly lower (P<0.05). This may explain the poor outcomes noted in the high-risk group of patients with OS.

Some of these five genes involved in the signature have already been studied by a number of studies. MAPK1 encodes a member of the MAP kinase family, which serves as an integration point for various biochemical signals involved in several cellular processes, such as proliferation, differentiation, transcriptional regulation, and development. The study by Wu *et al* indicated that microRNA (miR)-511 mimics inhibited OS cell proliferation and invasion, and reduced tumor load in metastatic OS in nude mice by targeting MAPK1 (29).

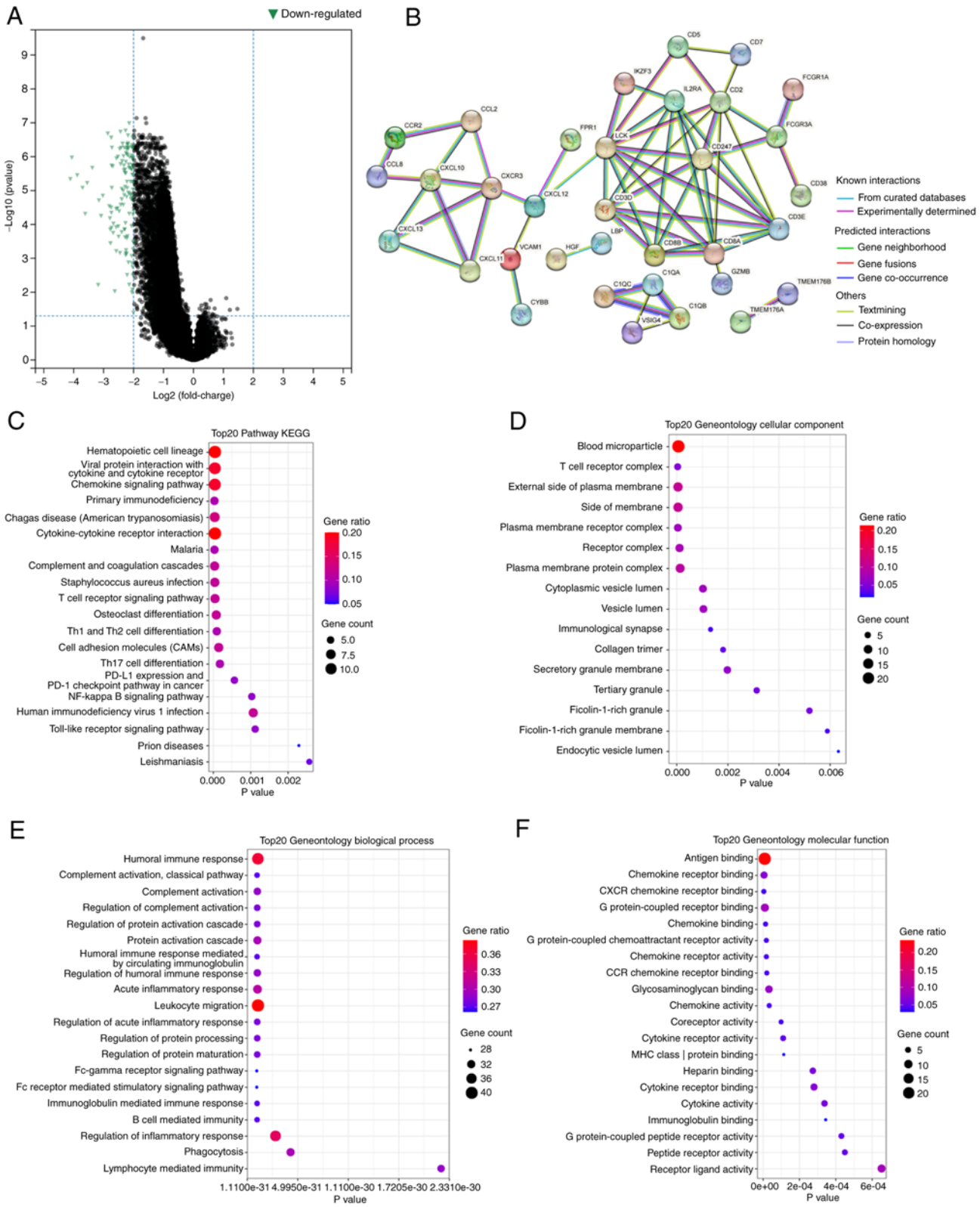

Figure 5. Identification and functional analysis of DEGs in high-risk group. (A) Volcano map of DEGs. (B) Construction of protein-protein interaction network based on the top 100 down-regulated genes. (C) KEGG bubble plot showed the top 20 enriched pathways of DEGs. The top 20 enriched functions of DEGs in GO including (D) cellular component, (E) biological process and (F) molecular function. DEGs, differentially expressed genes; KEGG, Kyoto Encyclopedia of Genes and Genomes.

Although G6PD is a relatively well-known gene, its role in the development of OS remains understudied. Wang *et al* demonstrated that long non-coding RNA OR3A4 regulated the growth of OS cells by regulating miR-1207-5p/G6PD signaling (30). Chemokines are a family of secreted proteins involved in immune regulation and inflammatory processes. It has been shown that CCL2 is highly expressed in OS and acts by promoting the proliferation and invasion of OS cells via the

Table II. Detailed information of hub OXSRGs.

Gene symbols	Full names	Log_2FC	FDR	Coefficient
CAT	Catalase	-1.03	<0.001	-0.018
MAPK1	Mitogen-Activated Protein Kinase 1	-0.84	<0.001	-0.019
G6PD	Glucose-6-Phosphate Dehydrogenase	-1.26	<0.001	-0.165
MAP3K5	Mitogen-Activated Protein Kinase Kinase Kinase 5	-1.68	<0.001	-0.215
CCL2	C-C Motif Chemokine Ligand 2	-2.42	<0.001	-0.120

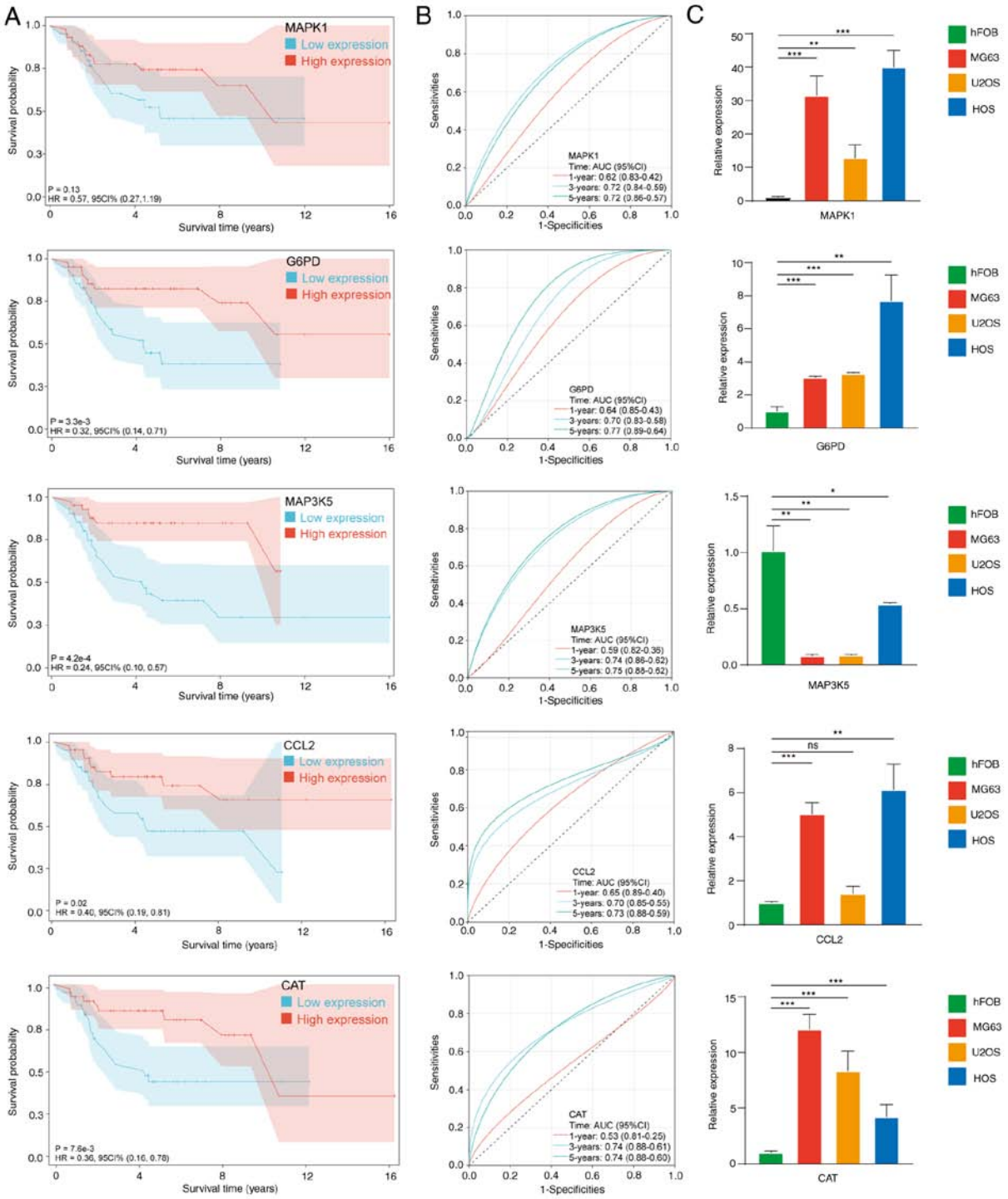

Figure 6. Single gene analysis in TARGET cohort. (A) Kaplan-Meier survival analysis of five hub OXSRGs. (B) Receiver operator curves demonstrated the predictive prognostic value of five hub OXSRGs. (C) PCR demonstrated differential expression of five hub OXSRGs in osteosarcoma. *P<0.05, **P<0.01, ***P<0.001. OXSRGs, oxidative stress-related genes; G6PD, glucose-6-phospate dehydrogenase; CCL2, chemokine ligand 2; CAT, catalase.

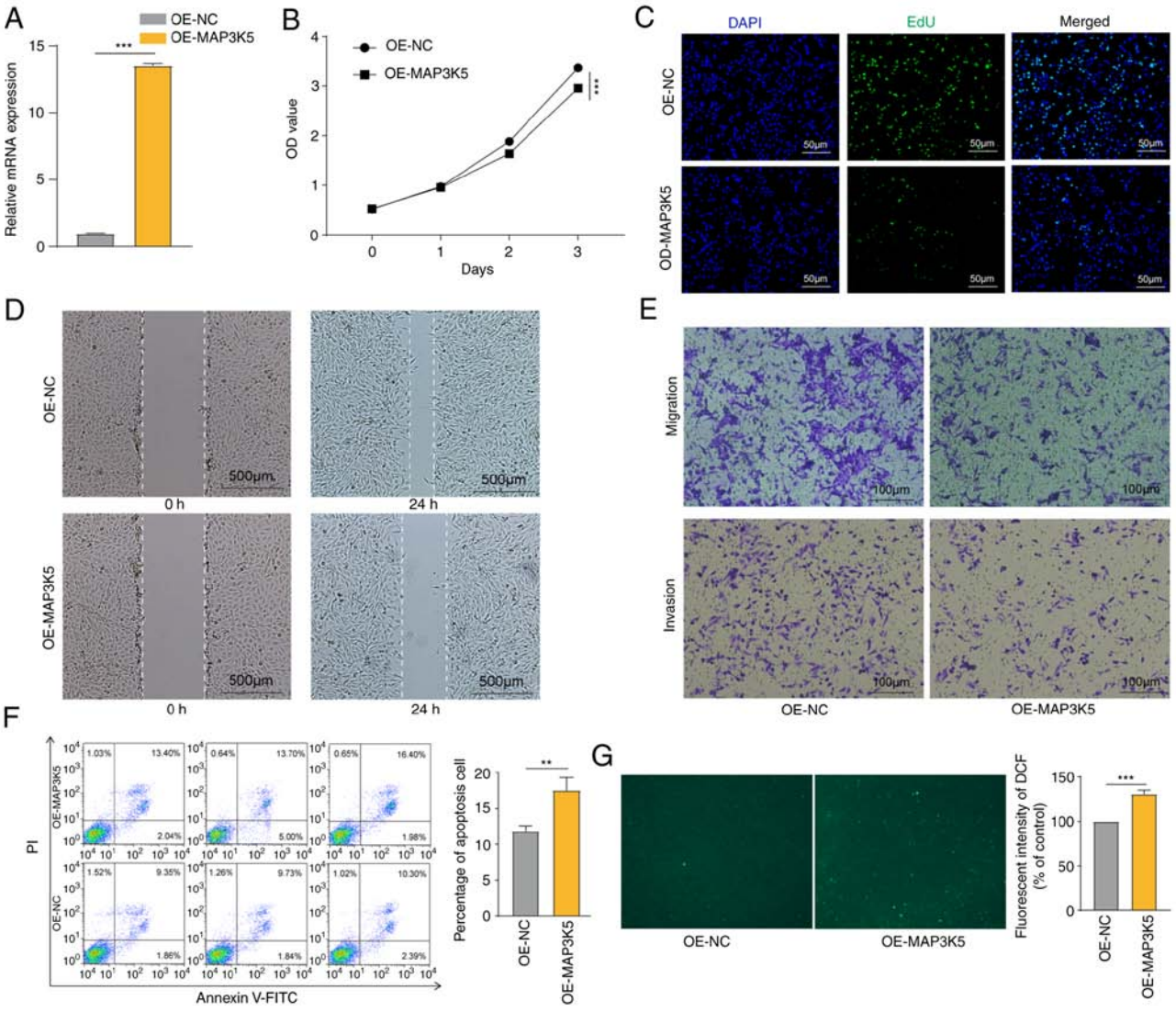

Figure 7. Inhibitory effect of MAP3K5 on osteosarcoma cells. (A) Construction of osteosarcoma cell lines overexpressing MAP3K5. (B) Cell proliferation was detected by measuring the optical intensity in 450 nm. (C) EdU staining (green fluorescence) on cell proliferation, 3 days after the construction of osteosarcoma cell lines overexpressing MAP3K5, nuclei were counterstained blue with DAPI (scale bars, 50 μm). (D) Representative images of wound healing assays after 24 h of the gap formation (scale bars, 500 μm). (E) Representative images of Transwell assays (migration and invasion) after 24 h incubation (scale bars, 100 μm). (F) Percentage of cell apoptosis was assessed via flow cytometry. (G) ROS production was assessed by measuring the fluorescent intensity of DCF on a fluorescent plate reader. Incremental production of ROS was expressed as a percentage of control. **P<0.01 and ***P<0.001. OE-NC, normal control (empty plasmid); ROS, reactive oxygen species; OE, overexpression.

receptor activator of nuclear factor kappa-B ligand signaling pathway (31).

Several studies have been published reporting the role of MAP3K5 in various human diseases (32,33). Currently, MAP3K5 has been identified as one of the key components in the regulation of ROS (34). Activation of MAP3K5 can produce pro-inflammatory cytokines, which are critical to the innate immune response (35). However, a limited number of studies have focused on the association of MAP3K5 with OS. OS. Gao *et al* demonstrated that miR-494 repressed OS development by modulating the formation of MAP3K5-related apoptosis complexes (36). In the present study, molecular experiments were performed to further investigate the role of MAP3K5 in OS. The data revealed that MAP3K5 was a negative factor to OS. Patients with high expression of MAP35 had higher survival rates. MAP3K5 exhibited inhibitory effects on OS cells. In addition, MAP3K5 induced ROS generation in OS cells.

However, certain limitations are evident in the present study. Firstly, the total number of patients with OS in the present study was limited and future studies require a larger dataset to further validate this prediction model. Secondly, biological experiments are required to investigate the molecular mechanisms by which OXSRGs affect OS prognosis. Importantly, bioinformatic methods were applied in interpreting these results in the data and presenting the new findings of the current study. These results are, to some extent, enlightening for subsequent mechanistic studies.

In the current study, an OXSRG signature was developed and validated to predict the prognosis of patients with OS, which provided a novel idea for the treatment of OS. It was also discovered that MAP3K5 may be a therapeutic target of OS. The detection of MAP3K5 expression in the osteosarcoma tissue of patients is a limitation of our study and an aim of future experiments.

Acknowledgements

Not applicable.

Funding

No funding was received.

Availability of data and materials

The data generated during and/or analyzed during the current study are available from the corresponding author upon reasonable request.

Authors' contributions

JL planned the study and supervised the analyses. BX collected data, performed the experiments and analyses. ST and CL drafted the manuscript and have made significant contributions to the analysis and interpretation of the data. JL and BX confirm the authenticity of all the raw data. All authors read and approved the final version of the manuscript.

Ethics approval and consent to participate

Not applicable.

Patient consent for publication

Not applicable.

Competing interests

The authors declare that they have no competing interests.

References

1. Kansara M, Teng MW, Smyth MJ and Thomas DM: Translational biology of osteosarcoma. Nat Rev Cancer 14: 722-735, 2014.
2. Wang T, Wang L, Zhang L, Long Y, Zhang Y and Hou Z: Single-cell RNA sequencing in orthopedic research. Bone Res 11: 10, 2023.
3. Wu CC and Livingston JA: Genomics and the immune landscape of osteosarcoma. Adv Exp Med Biol 1258: 21-36, 2020.
4. Sun W, Wang B, Qu XL, Zheng BQ, Huang WD, Sun ZW, Wang CM and Chen Y: Metabolism of reactive oxygen species in osteosarcoma and potential treatment applications. Cells 9: 87, 2019.
5. Liu W, Zhao Y, Wang G, Feng S, Ge X, Ye W, Wang Z, Zhu Y, Cai W, Bai J and Zhou X: TRIM22 inhibits osteosarcoma progression through destabilizing NRF2 and thus activation of ROS/AMPK/mTOR/autophagy signaling. Redox Biol 53: 102344, 2022.
6. Sarmiento-Salinas FL, Perez-Gonzalez A, Acosta-Casique A, Ix-Ballote A, Diaz A, Treviño S, Rosas-Murrieta NH, Millán-Perez-Peña L and Maycotte P: Reactive oxygen species: Role in carcinogenesis, cancer cell signaling and tumor progression. Life Sci 284: 119942, 2021.
7. Cheung EC and Vousden KH: The role of ROS in tumour development and progression. Nat Rev Cancer 22: 280-297, 2022.
8. Roy K, Wu Y, Meitzler JL, Juhasz A, Liu H, Jiang G, Lu J, Antony S and Doroshow JH: NADPH oxidases and cancer. Clin Sci (Lond) 128: 863-875, 2015.
9. García JG, Ansorena E, Izal I, Zalba G, de Miguel C and Milagro FI: Structure, regulation, and physiological functions of NADPH oxidase 5 (NOX5). J Physiol Biochem, Mar 11, 2023 (Epub ahead of print).
10. Moloney JN, Stanicka J and Cotter TG: Subcellular localization of the FLT3-ITD oncogene plays a significant role in the production of NOX- and $p22^{phox}$-derived reactive oxygen species in acute myeloid leukemia. Leuk Res 52: 34-42, 2017.
11. Sabharwal SS and Schumacker PT: Mitochondrial ROS in cancer: Initiators, amplifiers or an Achilles' heel? Nat Rev Cancer 14: 709-721, 2014.
12. Marcucci G, Domazetovic V, Nediani C, Ruzzolini J, Favre C and Brandi ML: Oxidative stress and natural antioxidants in osteoporosis: Novel preventive and therapeutic approaches. Antioxidants (Basel) 12: 373, 2023.
13. Bai H, Chen G, Fang C, Yang X, Yu S and Hai C: Osteosarcoma cell proliferation and migration are partly regulated by redox-activated NHE-1. J Clin Transl Res 1: 168-179, 2015.
14. Shin SH, Choi YJ, Lee H, Kim HS and Seo SW: Oxidative stress induced by low-dose doxorubicin promotes the invasiveness of osteosarcoma cell line U2OS in vitro. Tumour Biol 37: 1591-1598, 2016.
15. Warde-Farley D, Donaldson SL, Comes O, Zuberi K, Badrawi R, Chao P, Franz M, Grouios C, Kazi F, Lopes CT, *et al*: The GeneMANIA prediction server: Biological network integration for gene prioritization and predicting gene function. Nucleic Acids Res 38: W214-W220, 2010.
16. Yu G, Wang LG, Han Y and He QY: clusterProfiler: An R package for comparing biological themes among gene clusters. OMICS 16: 284-287, 2012.
17. R-Forge: estimate: Estimate of stromal and immune cells in malignant tumor tissues from expression data. https://R-Forge.R-project.org/projects/estimate/.
18. Ritchie ME, Phipson B, Wu D, Hu Y, Law CW, Shi W and Smyth GK: limma powers differential expression analyses for RNA-sequencing and microarray studies. Nucleic Acids Res 43: e47, 2015.
19. Zhang L, Jiao G, Ren S, Zhang X, Li C, Wu W, Wang H, Liu H, Zhou H and Chen Y: Exosomes from bone marrow mesenchymal stem cells enhance fracture healing through the promotion of osteogenesis and angiogenesis in a rat model of nonunion. Stem Cell Res Ther 11: 38, 2020.
20. Zheng D, Xia K, Yu L, Gong C, Shi Y, Li W, Qiu Y, Yang J and Guo W: A novel six metastasis-related prognostic gene signature for patients with osteosarcoma. Front Cell Dev Biol 9: 699212, 2021.
21. Morgan MJ and Liu ZG: Crosstalk of reactive oxygen species and NF-κB signaling. Cell Res 21: 103-115, 2011.
22. Sun SC: The noncanonical NF-κB pathway. Immunol Rev 246: 125-140, 2012.
23. Sahoo BM, Banik BK, Borah P and Jain A: Reactive oxygen species (ROS): Key components in cancer therapies. Anticancer Agents Med Chem 22: 215-222, 2022.
24. Parkinson EK, Haferkamp S and Mycielska ME: Cancer cell metabolism. Int J Mol Sci 23: 7210, 2022.
25. Pavlova, NN, Zhu J and Thompson CB: The hallmarks of cancer metabolism: Still emerging. Cell Metab 34: 355-377, 2022.
26. Diehn M, Cho RW, Lobo NA, Kalisky T, Dorie MJ, Kulp AN, Qian D, Lam JS, Ailles LE, Wong M, *et al*: Association of reactive oxygen species levels and radioresistance in cancer stem cells. Nature 458: 780-783, 2009.
27. Babior BM, Kipnes RS and Curnutte JT: Biological defense mechanisms. The production by leukocytes of superoxide, a potential bactericidal agent. J Clin Invest 52: 741-744, 1973.
28. Yang Y, Bazhin AV, Werner J and Karakhanova S: Reactive oxygen species in the immune system. Int Rev Immunol 32: 249-270, 2013.
29. Wu J, Zhang C and Chen L: MiR-511 mimic transfection inhibits the proliferation, invasion of osteosarcoma cells and reduces metastatic osteosarcoma tumor burden in nude mice via targeting MAPK1. Cancer Biomark 26: 343-351, 2019.
30. Wang X, Chen K and Zhao Z: LncRNA OR3A4 regulated the growth of osteosarcoma cells by modulating the miR-1207-5p/G6PD signaling. Onco Targets Ther 13: 3117-3128, 2020.
31. Chen Q, Sun W, Liao Y, Zeng H, Shan L, Yin F, Wang Z, Zhou Z, Hua Y and Cai Z: Monocyte chemotactic protein-1 promotes the proliferation and invasion of osteosarcoma cells and upregulates the expression of AKT. Mol Med Rep 12: 219-225, 2015.
32. Challa TD, Wueest S, Lucchini FC, Dedual M, Modica S, Borsigova M, Wolfrum C, Blüher M and Konrad D: Liver ASK1 protects from non-alcoholic fatty liver disease and fibrosis. EMBO Mol Med 11: e10124, 2019.

33. Zhao H, Chen X, Hu G, Li C, Guo L, Zhang L, Sun F, Xia Y, Yan W, Cui Z, *et al*: Small extracellular vesicles from brown adipose tissue mediate exercise cardioprotection. Circ Res 130: 1490-1506, 2022.
34. Ichijo H, Nishida E, Irie K, ten Dijke P, Saitoh M, Moriguchi T, Takagi M, Matsumoto K, Miyazono K and Gotoh Y: Induction of apoptosis by ASK1, a mammalian MAPKKK that activates SAPK/JNK and p38 signaling pathways. Science 275: 90-94, 1997.
35. Matsuzawa A, Saegusa K, Noguchi T, Sadamitsu C, Nishitoh H, Nagai S, Koyasu S, Matsumoto K, Takeda K and Ichijo H: ROS-dependent activation of the TRAF6-ASK1-p38 pathway is selectively required for TLR4-mediated innate immunity. Nat Immunol 6: 587-592, 2005.
36. Gao G and Jian Y: MicroRNA-494 represses osteosarcoma development by modulating ASK-1 related apoptosis complexes. Transl Cancer Res 9: 4121-4130, 2020.